

Fractional Order Computing and Modeling with Portending Complex Fit Real-World Data

Yeliz Karaca[1,2(✉)], Mati ur Rahman[3], and Dumitru Baleanu[4,5]

[1] University of Massachusetts Chan Medical School (UMASS), 55 Lake Avenue North, Worcester, MA 01655, USA
yeliz.karaca@ieee.org
[2] Massachusetts Institute of Technology (MIT), 77 Massachusetts Avenue, Cambridge, MA 02139, USA
[3] Department of Computer Science and Mathematics, Lebanese American University, Beirut, Lebanon
[4] Department of Mathematics, Çankaya University, 1406530 Ankara, Türkiye
[5] Institute of Space Sciences, Magurele, Bucharest, Romania

Abstract. Fractional computing models identify the states of different systems with a focus on formulating fractional order compartment models through the consideration of differential equations based on the underlying stochastic processes. Thus, a systematic approach to address and ensure predictive accuracy allows that the model remains physically reasonable at all times, providing a convenient interpretation and feasible design regarding all the parameters of the model. Towards these manifolding processes, this study aims to introduce new concepts of fractional calculus that manifest crossover effects in dynamical models. Piecewise global fractional derivatives in sense of Caputo and Atangana-Baleanu-Caputo (ABC) have been utilized, and they are applied to formulate the Zika Virus (ZV) disease model. To have a predictive analysis of the behavior of the model, the domain is subsequently split into two subintervals and the piecewise behavior is investigated. Afterwards, the fixed point theory of Schauder and Banach is benefited from to prove the existence and uniqueness of at least one solution in both senses for the considered problem. As for the numerical simulations as per the data, Newton interpolation formula has been modified and extended for the considered nonlinear system. Finally, graphical presentations and illustrative examples based on the data for various compartments of the systems have been presented with respect to the applicable real-world data for different fractional orders. Based on the impact of fractional order reducing the abrupt changes, the results obtained from the study demonstrate and also validate that increasing the fractional order brings about a greater crossover effect, which is obvious from the observed data, which is critical for the effective management and control of abrupt changes like infectious diseases, viruses, among many more unexpected phenomena in chaotic, uncertain and transient circumstances.

© The Author(s), under exclusive license to Springer Nature Switzerland AG 2023
O. Gervasi et al. (Eds.): ICCSA 2023 Workshops, LNCS 14104, pp. 144–159, 2023.
https://doi.org/10.1007/978-3-031-37105-9_11

Keywords: Fractional computing models · crossover behavior · complex fit real-world data · mathematical biology · computational biology · fractional calculus · piecewise global fractional derivatives · Newton interpolation formula · ABC fractional derivatives · equicontinuous mapping · Schauder's fixed point theorem · dynamics of multi-compartment models · fractional order compartment models · stochastic differential equations · differential equations

1 Introduction

The integration of advanced mathematics towards the solution of fractional-order calculus/systems and achieve the feasible designs for various applications of fractional-order systems. Accordingly, fractional-order modeling of dynamic systems with applications is utilized to describe various real-world phenomena and processes. Dynamical systems are often modeled based on algebraic, differential/integral or difference equations, while the majority of real-world processes as well as phenomena have been modeled by using nonlinear differential or integral and difference equations. This particular domain has diverse applications in most fields of engineering, physics, chemistry, control theory, mathematical biology and epidemiology. Several illnesses and viral diseases have significantly affected human populations, ranging from measles, to TB, malaria, HBV, HCV, tumor cancers, the Spanish flu and COVID-19, among many others, resulting in high mortality rates.

As a result of such abrupt developments, various strategies have been designed and implemented to control and reduce the spread of infections within their communities. While many epidemics have been effectively controlled through the discovery of cures and treatments, there are still some diseases that remain incurable and lack proper medications or treatments. Among the aforesaid diseases, Zika disease, is one of the most infectious ones, caused by the bite of infectious Aedes insects. Outbreaks due to Zika virus have been recorded in different counties of Africa (for further details please see [1]). The symptoms of disease are laziness and sudden disease cause other signs like rashes of skins, sudden fever, conjunctness and feeling of pains in all parts of the body. The said signs may remain for two to seven days, and sometimes the signs do not appear in the infecting individual. This virus may also impact all the women whom have pregnancy and may transferred to the new born easily (see further detail in [2,3]). In this way, the new fetal may also faces abnormality, small head, weak muscles and weak system of nerves.

It is remarkable that researchers are increasingly use different tools and analysis for investigating epidemiological disease, and one of the powerful tools is the mathematical formulation. Mathematical models have been increasingly used as robust means for the predictions and accurate analyses pertaining to the transmission dynamics of infectious diseases. Given these, varying degrees of mathematical models have been formulated, used for the description of different diseases. Different studies have provided the formulation of the ZV disease by using nonlinear differential equations. For instance, the Kucharsk et al. [4] formulated

the ZV disease which spread during 2013–14 in France. By the applications of controlling theory of optimality, Okosun and Bonyah [5] investigated some procedural means to minimize the transition dynamics of the infection, and another study posited that the usage of cure and spray for mosquitos could reduce its spread (see the details in [6]). For some remarkable applications of fractional differential operators, the following references can be referred to [7–9]. It should be noted that fractional order integral and differential operators are nonlocal in nature and have the ability to provide global dynamics which include the traditional order dynamics as special case (see further details in [10,11]). As a result of the aforementioned observations, researchers have been prompted to investigate various dynamic problems in the context of fractional order derivatives utilizing different operators, as evident in [12–14].

There are differential operators of two classes of operators on the basis of kernels: while one class includes operators such as Riemann-Liouville and Caputo operators with singular kernel type operators, others such as Caputo-Fabrizio and Atangana-Baleanu, many others, are included in non-singular kernel type class. It can be stated that both kinds have a variety of applications in mathematical modeling of various real-world problems, having been used in many studies some of which are in [15–17]. To study the phenomenon of crossover behavior, numerous differential operators have been proposed in the literature, such as fractal derivatives, non-integer order derivatives with singular or non-singular kernels, fractal-fractional operators, among many others (see [19–21] for more details). Although randomness can be modeled using stochastic equations with some degree of success, the phenomenon of crossover behavior in dynamics remains a challenging problem to explain. In the field of fractional calculus, exponential and Mittag-Leffler mappings have limitations in determining the time of crossovers. To address this issue, new approaches involving various piecewise differentiations and integrations have recently been introduced (see [22] for more details). In this paper, we provide an introduction of classical and global piecewise derivatives and integral, along with some applicable examples and numerical schemes with feasible design. Towards these manifolding processes, this study, with the unique solution of the proposed problem, aims to introduce new concepts of fractional calculus that manifest crossover effects in dynamical models. In addition, as inspired from the above discussion, we initially investigate the mathematical model given in [18] by using the Caputo and Atangana-Baleanu piecewise differential operators. We formulated the proposed model in the

$$
\begin{aligned}
&{}_0^{CABC}D_t^{\varpi}(\mathcal{X}(t)) = \lambda_h - \alpha_1\beta_1\mathcal{X}\mathcal{U} - \delta_1\mathcal{X},\\
&{}_0^{CABC}D_t^{\varpi}(\mathcal{Y}(t)) = \alpha_1\beta_1\mathcal{X}\mathcal{U} - \delta_1\mathcal{Y},\\
&{}_0^{CABC}D_t^{\varpi}(\mathcal{Z}(t)) = \lambda_m - \alpha_2\beta_2\mathcal{Y}\mathcal{Z} - \delta_2\mathcal{Z},\\
&{}_0^{CABC}D_t^{\varpi}(\mathcal{U}(t)) = \alpha_2\beta_2\mathcal{Y}\mathcal{Z} - \delta_2\mathcal{U},\\
&\mathcal{X}(0) = \mathcal{X}_0,\ \mathcal{Y}(0) = \mathcal{Y}_0,\\
&\mathcal{Z}(0) = \mathcal{Z}_0,\ \mathcal{U}(0) = \mathcal{U}_0,
\end{aligned}
\tag{1}
$$

In a more explicit form, the model (1) can also be written as

$$
\begin{aligned}
{}_0^{CABC}D_t^{\varpi}(\mathcal{X}(t)) &= \begin{cases} {}_0^{C}D_t^{\varpi}(\mathcal{X}(t)) = {}^{C} H_1(\mathcal{X},\mathcal{Y},\mathcal{Z},\mathcal{U},t), & 0 < t \le t_1, \\ {}_0^{ABC}D_t^{\varpi}(\mathcal{X}(t)) = {}^{ABC} H_1(\mathcal{X},\mathcal{Y},\mathcal{Z},\mathcal{U},t), & t_1 < t \le T, \end{cases} \\
{}_0^{CABC}D_t^{\varpi}(\mathcal{Y}(t)) &= \begin{cases} {}_0^{C}D_t^{\varpi}(\mathcal{Y}(t)) = {}^{C} H_2(\mathcal{X},\mathcal{Y},\mathcal{Z},\mathcal{U},t), & 0 < t \le t_1, \\ {}_0^{ABC}D_t^{\varpi}(\mathcal{Y}(t)) = {}^{ABC} H_2(\mathcal{X},\mathcal{Y},\mathcal{Z},\mathcal{U},t), & t_1 < t \le T, \end{cases} \\
{}_0^{CABC}D_t^{\varpi}(\mathcal{Z}(t)) &= \begin{cases} {}_0^{C}D_t^{\varpi}(\mathcal{Z}(t)) = {}^{C} H_3(\mathcal{X},\mathcal{Y},\mathcal{Z},\mathcal{U},t), & 0 < t \le t_1, \\ {}_0^{ABC}D_t^{\varpi}(\mathcal{Z}(t)) = {}^{ABC} H_3(\mathcal{X},\mathcal{Y},\mathcal{Z},\mathcal{U},t), & t_1 < t \le T, \end{cases} \\
{}_0^{CABC}D_t^{\varpi}(\mathcal{U}(t)) &= \begin{cases} {}_0^{C}D_t^{\varpi}(\mathcal{U}(t)) = {}^{C} H_4(\mathcal{X},\mathcal{Y},\mathcal{Z},\mathcal{U},t), & 0 < t \le t_1, \\ {}_0^{ABC}D_t^{\varpi}(\mathcal{U}(t)) = {}^{ABC} H_4(\mathcal{X},\mathcal{Y},\mathcal{Z},\mathcal{U},t), & t_1 < t \le T, \end{cases}
\end{aligned} \tag{2}
$$

where ${}_0^{C}D_t^{\varpi}$ and ${}_0^{ABC}D_t^{\varpi}$ are Caputo and ABC derivative respectively. We investigate the existence results and uniqueness of at least one approximate solution.

The remainder of this paper is outlined as follows: Sect. 2 provides Preliminary definitions, Sect. 3 presents information on Existence and uniqueness demonstrative results and Sect. 4 on Numerical Scheme. The next section, namely Sect. 5, addresses Experimental Results and Discussion: Numerical performances of the piecewise global fractional derivatives for Zika virus infection and finally Sect. 6 provides Conclusion and Future Directions.

2 Preliminary Definitions

Foundational definitions can be provided in this part of the study [19,21].

Definition 1. *Let $V(t) \in \mathcal{H}^1(0,T)$ be a function, the ABC derivative can be written as*

$$
{}^{ABC}{}_0D_t^{\varpi}(V(t)) = \frac{ABC(\varpi)}{1-\varpi}\int_0^t \frac{d}{d\wp}V(\wp)E_{\varpi}\left[\frac{-\varpi}{1-\varpi}\left(t-\wp\right)^{\varpi}\right]d\wp, \tag{3}
$$

where the normalization function is defined as $ABC(0) = ABC(1) = 1$.

And the integration can be written as

$$
{}^{ABC}{}_0I_t^{\varpi}V(t) = \frac{1-\varpi}{ABC(\varpi)}V(t) + \frac{\varpi}{ABC(\varpi)\Gamma(\varpi)}\int_0^t (t-\wp)^{\varpi-1}V(\wp)d\wp. \tag{4}
$$

Definition 2. *The Caputo derivative for a function $V(t)$ is defined as*

$$
{}_0^{C}D_t^{\varpi}V(t) = \frac{1}{\Gamma(1-\varpi)}\int_0^t (t-\wp)^{n-\varpi-1}[V^{'}(\wp)]d\wp.
$$

Definition 3. *Consider a differentiable increasing functions be $V(t)$ and $g(t)$, then the classical piecewise derivative is given as*

$$ {}_0^{PG}D_t V(t) = \begin{cases} V(t), & 0 < t \leq t_1, \\ \dfrac{V'(t)}{g'(t)} & t_1 < t \leq T, \end{cases} $$

while the integration is

$$ {}_0^{PG}I_t V(t) = \begin{cases} \displaystyle\int_0^t V(\tau)d\tau, & 0 < t \leq t_1, \\ \displaystyle\int_{t_1}^t V(\tau)g'(\tau)d(\tau) & t_1 < t \leq T, \end{cases} $$

here ${}_0^{PG}D_t V(t)$ and ${}_0^{PG}I_t V(t)$ stands for classical derivative and integration in $0 < t \leq t_1$ and for global derivative and integration in $t_1 < t \leq T$.

Definition 4. *Consider a differentiable function be $V(t)$, then the classical and fractional piecewise derivative is defined as*

$$ {}_0^{PC}D_t^{\varpi} V(t) = \begin{cases} V'(t), & 0 < t \leq t_1, \\ {}_0^{C}D_t^{\varpi} V(t) & t_1 < t \leq T, \end{cases} $$

and the integration can be written as

$$ {}_0^{PC}I_t V(t) = \begin{cases} \displaystyle\int_0^t V(\tau)d\tau, & 0 < t \leq t_1, \\ \dfrac{1}{\Gamma\varpi}\displaystyle\int_{t_1}^t (t-\wp)^{\varpi-1} V(\wp)d(\wp) & t_1 < t \leq T, \end{cases} $$

here ${}_0^{PC}D_t^{\varpi} V(t)$ and ${}_0^{PC}I_t V(t)$ present classical derivative and integration in $0 < t \leq t_1$ and fractional derivative and integration in $t_1 < t \leq T$.

Definition 5. *If a differentiable function be $V(t)$, then the Caputo and ABC piecewise derivative is given by*

$$ {}_0^{PCABC}D_t^{\varpi} V(t) = \begin{cases} {}_0^{C}D_t^{\varpi} V(t), & 0 < t \leq t_1, \\ {}_0^{ABC}D_t^{\varpi} V(t) & t_1 < t \leq T, \end{cases} $$

while the integration can be written as

$$ {}_0^{PCABC}I_t V(t) = \begin{cases} \dfrac{1}{\Gamma\varpi}\displaystyle\int_{t_1}^t (t-\wp)^{\varpi-1} V(\wp)d(\wp), & 0 < t \leq t_1, \\ \dfrac{1-\varpi}{ABC\varpi} V(t) + \dfrac{\varpi}{ABC\varpi\Gamma\varpi}\displaystyle\int_{t_1}^t (t-\wp)^{\varpi-1} V(\wp)d(\wp) & t_1 < t \leq T. \end{cases} $$

here ${}_0^{PCABC}D_t^{\varpi} V(t)$ and ${}_0^{PCABC}I_t V(t)$ is Caputo derivative and integration in $0 < t \leq t_1$ and ABC derivative and integration in $t_1 < t \leq T$.

Lemma 1. *The piecewise derivable equation solution for the right sides vanishes at* $t = 0$

$$ {}_{0}^{PCABC}D_{t}^{\varpi}\mathcal{V}(t) = H(\mathcal{V}, t), \quad 0 < \varpi \leq 1 $$

is given by

$$ \mathcal{V}(t) = \begin{cases} \mathcal{V}_0 + \dfrac{1}{\Gamma(\varpi)} \displaystyle\int_0^t H(\wp, \mathcal{V}(\wp))(t-\wp)^{\varpi-1} d\wp, \ 0 < t \leq t_1 \\ \mathcal{V}(t_1) + \dfrac{1-\varpi}{ABC(\varpi)} H(\mathcal{V}, t) + \dfrac{\varpi}{ABC(\varpi)\Gamma(\varpi)} \displaystyle\int_{t_1}^t (t-\wp)^{\varpi-1} H(\wp, \mathcal{V}(\wp)) d(\wp). \end{cases} $$

3 Existence and Uniqueness Demonstrative Results

In order to demonstrate the existence and uniqueness of a solution to the problem at hand, we can express the system can be stated (2) in a manner similar to that shown in Lemma 1. Building on this, we can then proceed to provide a more detailed explanation, as follows, can be provided:

$$ {}_{0}^{PCABC}D_{t}^{\varpi}\mathcal{V}(t) = H(t, \mathcal{V}(t)), \quad 0 < \varpi \leq 1, $$

is

$$ \mathcal{V}(t) = \begin{cases} \mathcal{V}_0 + \dfrac{1}{\Gamma(\varpi)} \displaystyle\int_0^t H(\wp, \mathcal{V}(\wp))(t-\wp)^{\varpi-1} d\wp, \ 0 < t \leq t_1, \\ \mathcal{V}(t_1) + \dfrac{1-\varpi}{ABC(\varpi)} H(\mathcal{V}, t) + \dfrac{\varpi}{ABC(\varpi)\Gamma\varpi} \displaystyle\int_{t_1}^t (t-\wp)^{\varpi-1} H(\wp, \mathcal{V}(\wp)) d(\wp), \end{cases} \tag{5} $$

where

$$ \mathcal{V}(t) = \begin{cases} X(t) \\ Y(t) \\ Z(t) \\ U(t), \end{cases} \quad \mathcal{V}_0 = \begin{cases} X_0 \\ Y_0 \\ Z_0 \\ U_0, \end{cases} \quad \mathcal{V}_{t_1} = \begin{cases} X_{t_1} \\ Y_{t_1} \\ Z_{t_1} \\ U_{t_1}, \end{cases} \quad H(t, \mathcal{V}(t)) = \left\{ H_i = \begin{cases} {}^{C}H_i(\mathcal{X}, \mathcal{Y}, \mathcal{Z}, \mathcal{U}, t) \\ {}^{ABC}H_i(\mathcal{X}, \mathcal{Y}, \mathcal{Z}, \mathcal{U}, t), \end{cases} \right. \tag{6} $$

where $i = 1, 2, 3, 4$. Take $\infty > T \geq t > 0$ with Banach space as $E_1 = C[0, T]$ endowed with norm

$$ \|\mathcal{V}\| = \max_{t \in [0,T]} |\mathcal{V}(t)|. $$

In order to obtain the desired outcome, we examine the growth condition of the non-linear function, which can be expressed as:

(C1) There exists constants $L_{\mathcal{V}} > 0$; for every H, $\bar{\mathcal{V}} \in E \ni$

$$ |H(t, \mathcal{V}) - H(t, \bar{\mathcal{V}})| \leq L_H |\mathcal{V} - \bar{\mathcal{V}}|. $$

(C2) Let one has constants $C_H > 0$ and $M_H > 0$, $\ni$

$$ |H(t, \mathcal{V})| \leq C_H |\mathcal{V}| + M_H $$

holds.

Theorem 1. *Assuming that H is continuous piecewisely on the subintervals $0 < t \leq t_1$ and $t_1 < t \leq T$ of $[0,T]$, and subject to the hypothesis $(C2)$, it can be concluded that the piecewise problem expressed in Eq. (2) has at least one solution on every of these subintervals.*

Proof. We can use the Schauder fixed point theorem to define a closed subset B of E on both subintervals $0 < T \leq t_1$ and $t_1 < T \leq T$.

$$B = \{\mathcal{V} \in E : \ \|\mathcal{V}\| \leq R_{1,2}, \ R_{1,2} > 0\},$$

Considering the operator $\mathcal{T} : B \to B$ and using Eq. (5) as

$$\mathcal{T}(\mathcal{V}) = \begin{cases} \mathcal{V}_0 + \frac{1}{\Gamma(\varpi)} \int_0^{t_1} H(\wp, \mathcal{V}(\wp))(t-\wp)^{\varpi-1} d\wp, \ 0 < t \leq t_1 \\ \mathcal{V}(t_1) + \frac{1-\varpi}{ABC(\varpi)} H(t, \mathcal{V}(t)) + \frac{\varpi}{ABC(\varpi)\Gamma(\varpi)} \int_{t_1}^{t} (t-\wp)^{\varpi-1} H(\wp\mathcal{V}(\wp)) d(\wp). \end{cases} \tag{7}$$

On any $\mathcal{V} \in B$, we get

$$\begin{aligned} |\mathcal{T}(\mathcal{V})(t)| &\leq \begin{cases} |\mathcal{V}_0| + \frac{1}{\Gamma(\varpi)} \int_0^{t_1} (t-\wp)^{\varpi-1} |H(\wp, \mathcal{U}(\wp))| d\wp, \\ |\mathcal{V}_{t_1}| + \frac{1-\varpi}{ABC(\varpi)} |H(t, \mathcal{V}(t))| \\ + \frac{\varpi}{ABC(\varpi)\Gamma(\varpi)} \int_{t_1}^{t} (t-\wp)^{\varpi-1} |H(\wp\mathcal{V}(\wp))| d(\wp), \end{cases} \\ &\leq \begin{cases} |\mathcal{V}_0| + \frac{\mathbf{T}^{\varpi}}{\Gamma(\varpi+1)} [C_H|\mathcal{V}| + M_H] = R_1, \ 0 < t \leq t_1, \\ |\mathcal{V}_{t_1}| + \frac{1-\varpi}{ABC(\varpi)} [C_H|\mathcal{V}| + M_H] \\ + \frac{\varpi(T-\mathbf{T})^{\varpi}}{ABC(\varpi)\Gamma\varpi+1} [C_H|\mathcal{V}| + M_H] d(\wp) = R_2, \end{cases} \\ \|\mathcal{T}(\mathcal{U})\| &\leq \begin{cases} R_1, \ 0 < t \leq t_1, \\ R_2, \ t_1 < t \leq T. \end{cases} \end{aligned}$$

Fixing $R_{1,2} = \max\{R_1, R_2\}$, we see that $\|\mathcal{T}(\mathcal{V})\| \leq R_{1,2}$ which demonstrate that $\mathcal{T}$ is bounded and also $\mathcal{T}(\mathcal{V}) \in B$. Thus, $\mathcal{T}(B) \subset B$. Further, for completely continuity, $t_i < t_j \in [0, t_1]$ is taken in Caputo sense such that

$$\begin{aligned} |\mathcal{T}(\mathcal{V})(t_j) - \mathcal{T}(\mathcal{V})(t_i)| &= \Big| \frac{1}{\Gamma(\varpi)} \int_0^{t_j} (t_j - \wp)^{\varpi-1} H(\wp, \mathcal{V}(\wp)) d\wp, \\ &\quad - \frac{1}{\Gamma(\varpi)} \int_0^{t_i} (t_i - \wp)^{\varpi-1} H(\wp, \mathcal{V}(\wp)) d\wp \Big| \\ &\leq \frac{(C_H\mathcal{V} + M_H)}{\Gamma(\varpi+1)} [t_j^{\varpi} - t_i^{\varpi} + 2(t_j - t_i)^{\varpi}]. \end{aligned} \tag{8}$$

From (8), it is observed that as t_i tends to t_j, then

$$|\mathcal{T}(\mathcal{V})(t_j) - \mathcal{T}(\mathcal{V})(t_i)| \to 0, \text{ as } t_i \to t_j.$$

Since $\mathcal{T}$ is bounded on $[0, t_1]$, so is uniformly continuous also over $[0, t_1]$. Hence, it can be concluded that $\mathcal{T}$ over the said interval is equi-continuous as well.

Next we take the other interval $t_i, t_j \in [t_1, T]$ in the ABC sense as

$$\begin{aligned}
&|\mathcal{T}(\mathcal{V})(t_j) - \mathcal{T}(\mathcal{V})(t_i)| = \Big| \frac{1-\varpi}{ABC(\varpi)} H(t, \mathcal{V}(t)) + \frac{\varpi}{ABC(\varpi)\Gamma(\varpi)} \int_{t_1}^{t_j} (t_j - \wp)^{\varpi-1} H(\wp, \mathcal{V}(\wp)) d\wp, \\
&- \frac{1-\varpi}{ABC(\varpi)} H(t, \mathcal{V}(t)) + \frac{(\varpi)}{ABC(\varpi)\Gamma(\varpi)} \int_{t_1}^{t_i} (t_i - \wp)^{\varpi-1} H(\wp, \mathcal{U}(\wp)) d\wp \Big| \qquad (9) \\
&\leq \frac{\varpi(C_H \mathcal{V} + M_H)}{ABC(\varpi)\Gamma(\varpi+1)} [t_j^{\varpi} - t_i^{\varpi} + 2(t_j - t_i)^{\varpi}].
\end{aligned}$$

Also from (9), we see that

$$|\mathcal{T}(\mathcal{V})(t_j) - \mathcal{T}(\mathcal{V})(t_i)| \to 0, \text{ as } t_i \to t_j.$$

Due to uniform continuity of $\mathcal{T}$ over the said interval, It can be concluded that the mapping $\mathcal{T}$ is equicontinuous over the interval $[t_1, T]$, making it an equicontinuous mapping. By applying the Arzelà-Ascoli theorem, it can be shown that the operator $\mathcal{T}$ is both completely continuous and uniformly continuous, and has bounds. Hence, using Schauder's fixed point theorem, it can be deduced that the piecewise differentiable problem stated in Eq. (2) has at least one solution on each subinterval.

Theorem 2. *In view of hypothesis* $(C1)$ *together with the condition that*

$$\max\left\{ \frac{\mathbf{T}^{\varpi}}{\Gamma(\varpi+1)} L_H, L_H \left[\frac{1-\varpi}{ABC(\varpi)} + \frac{\varpi(T-\mathbf{T})^{\varpi}}{ABC(\varpi)\Gamma(\varpi+1)} \right] \right\} < 1,$$

the proposed model has unique solution.

Proof. We define the operator $\mathcal{T} : E \to E$, where E is a certain set, and consider $\mathcal{V}$ and $\bar{\mathcal{V}} \in E$ on the interval $[0, t_1]$ in the Caputo sense

$$\begin{aligned}
\|\mathcal{T}(\mathcal{V}) - \mathcal{T}(\bar{\mathcal{V}})\| &= \max_{t \in [0,t_1]} \Big| \frac{1}{\Gamma(\varpi)} \int_0^t (t-\wp)^{\varpi-1} H(\wp, \mathcal{V}(\wp)) d\wp \\
&\quad - \frac{1}{\Gamma(\varpi)} \int_0^t (t-\wp)^{\varpi-1} H(\wp, \bar{\mathcal{V}}(\wp)) d\wp \Big| \\
&\leq \frac{\mathbf{T}^{\varpi}}{\Gamma(\varpi+1)} L_H \|\mathcal{V} - \bar{\mathcal{V}}\|.
\end{aligned}$$

Using Eq. (10), we obtain

$$\|\mathcal{T}(\mathcal{V}) - \mathcal{T}(\bar{\mathcal{V}})\| \leq \frac{\mathbf{T}^{\varpi}}{\Gamma(\varpi+1)} L_H \|\mathcal{V} - \bar{\mathcal{V}}\|. \qquad (10)$$

Assuming that $\mathcal{T}$ is a contraction, according to the Banach contraction theorem, the considered problem has a unique solution in the given sub-interval. For $t \in [t_1, T]$ and in the sense of the ABC derivative, we can proceed to the next step.

$$\|\mathcal{T}(\mathcal{V}) - \mathcal{T}(\bar{\mathcal{V}})\| \leq \frac{1-\varpi}{ABC(\varpi)} L_H \|\mathcal{V} - \bar{\mathcal{V}}\| + \frac{\varpi(\mathbf{T} - T^{\varpi})}{ABC(\varpi)\Gamma(\varpi+1)} L_H \|\mathcal{V} - \bar{\mathcal{V}}\|. \quad (11)$$

or

$$\|\mathcal{T}(\mathcal{V}) - \mathcal{T}(\bar{\mathcal{V}})\| \leq L_H \left[\frac{1-\varpi}{ABC(\varpi)} + \frac{\varpi(T - \mathbf{T})^{\varpi}}{ABC(\varpi)\Gamma(\varpi+1)} \right] \|\mathcal{V} - \bar{\mathcal{V}}\|. \quad (12)$$

Assuming that $\mathcal{T}$ is a contraction, we can apply the Banach contraction theorem to conclude that the considered problem has a unique solution in the given sub-interval. Furthermore, based on relations (10) and (12), it can be confirmed that the problem proposed in this study has a unique solution.

4 Numerical Scheme

In order to solve the system of piecewise differential equations given in Eq. (2), it is essential to design a numerical scheme, and accordingly, the approach of the study has been develop a scheme that works for the two subintervals, or strains, of the interval $[0, T]$, using the Caputo and ABC formulations. To achieve this, the numerical scheme for the piecewise derivative of integer order is handled, as has been presented in reference [22]. To apply the scheme, we use piecewise integration on the first Eq. (2), has been employed separately for the Caputo and ABC formats, which yields:

$$\mathcal{X}(t)) = \begin{cases} \mathcal{X}_0 + \dfrac{1}{\Gamma(\varpi)} \displaystyle\int_0^{t_1} (t-\wp)^{\varpi-1} {}^{C}H_1(\wp, \mathcal{X}) d\wp, \quad 0 < t \leq t_1, \\ \mathcal{X}(t_1) + \dfrac{1-\varpi}{ABC(\varpi)} {}^{ABC}H_1(t, \mathcal{X}) \\ + \dfrac{\varpi}{ABC(\varpi)\Gamma(\varpi)} \displaystyle\int_{t_1}^{t} (t-\wp)^{\varpi-1} {}^{ABC}H_1(\wp, \mathcal{X}) d\wp, \end{cases} \quad (13)$$

To obtain the numerical scheme for the system of equations given in (2), we will start with the first equation of the system is addressed, which is denoted by (13). It should be noted that the procedure we will describe can be repeated for the other compartments and partitions of the system as well.

At $t = t_{n+1}$, one has

$$\mathcal{X}(t_{n+1})) = \begin{cases} \mathcal{X}_0 + \dfrac{1}{\Gamma(\varpi)} \displaystyle\int_0^{t_1} (t-\wp)^{\varpi-1} {}^{C}H_1(\mathcal{X}, \wp) d\wp, \\ \mathcal{X}(t_1) + \dfrac{1-\varpi}{ABC(\varpi)} {}^{ABC}H_1(\mathcal{X}, t_n) \\ + \dfrac{\varpi}{ABC(\varpi)\Gamma(\varpi)} \displaystyle\int_{t_1}^{t_{n+1}} (t-\wp)^{\varpi-1} {}^{ABC}H_1(\wp, \mathcal{X}) d\wp. \end{cases} \quad (14)$$

Equation (14) can be presented using the Newton interpolation approximation, which is described in detail in reference [22].

$$\mathcal{X}(t_{n+1}) = \begin{cases} \mathcal{X}_0 + \begin{cases} \frac{(\Delta t)^{\varpi-1}}{\Gamma(\varpi+1)} \sum\limits_{k=2}^{i} \left[{}^{C}H_1(\mathcal{X}_{k-2}, t_{k-2}) \right] \Pi + \frac{(\Delta t)^{\varpi-1}}{\Gamma(\varpi+2)} \sum\limits_{k=2}^{i} \left[{}^{C}H_1(\mathcal{X}_{k-1}, t_{k-1}) \right. \\ \left. - {}^{C}H_1(\mathcal{X}_{k-2}, t_{k-2}) \right] \Sigma + \frac{\varpi(\Delta t)^{\varpi-1}}{2\Gamma(\varpi+3)} \sum\limits_{k=2}^{i} \left[{}^{C}H_1(\mathcal{X}_k, t_k) - 2^{C}H_1(\mathcal{X}_{k-1}, t_{k-1}) \right. \\ \left. + {}^{C}H_1(\mathcal{X}_{k-2}, t_{k-2}) \right] \Delta \\ \mathcal{X}(t_1) + \begin{cases} \frac{1-\varpi}{ABC(\varpi)} {}^{ABC}H_1(\mathcal{X}_n, t_n) + \frac{\varpi}{ABC(\varpi)} \frac{(\delta t)^{\varpi-1}}{\Gamma(\varpi+1)} \sum\limits_{k=i+3}^{n} \left[{}^{ABC}H_1(\mathcal{X}_{k-2}, t_{k-2}) \right] \Pi \\ + \frac{\varpi}{ABC(\varpi)} \frac{(\delta t)^{\varpi-1}}{\Gamma(\varpi+2)} \sum\limits_{k=i+3}^{n} \left[{}^{ABC}H_1(\mathcal{X}_{k-1}, t_{k-1}) + ABC H_1(\mathcal{X}_{k-2}, t_{k-2}) \right] \Sigma \\ + \frac{\varpi}{ABC(\varpi)} \frac{\varpi(\delta t)^{\varpi-1}}{\Gamma(\varpi+3)} \sum\limits_{k=i+3}^{n} \left[{}^{ABC}H_1(\mathcal{X}^k, t_k) - 2^{ABC}H_1(\mathcal{X}_{k-1}, t_{k-1}) \right. \\ \left. + {}^{ABC}H_1(\mathcal{X}_{k-2}, t_{k-2}) \right] \Delta. \end{cases} \end{cases} \tag{15}$$

Similarly, we can apply the Newton interpolation approximation can be applied to the remaining three compartments of the system of equations as well.

$$\mathcal{Y}(t_{n+1})) = \begin{cases} \mathcal{Y}_0 + \begin{cases} \frac{(\Delta t)^{\varpi-1}}{\Gamma(\varpi+1)} \sum\limits_{k=2}^{i} \left[{}^{C}H_2(\mathcal{Y}_{k-2}, t_{k-2}) \right] \Pi + \frac{(\Delta t)^{\varpi-1}}{\Gamma(\varpi+2)} \sum\limits_{k=2}^{i} \left[{}^{C}H_2(\mathcal{Y}_{k-1}, t_{k-1}) \right. \\ \left. - {}^{C}H_2(\mathcal{Y}_{k-2}, t_{k-2}) \right] \Sigma + \frac{\varpi(\Delta t)^{\varpi-1}}{2\Gamma(\varpi+3)} \sum\limits_{k=2}^{i} \left[{}^{C}H_2(\mathcal{Y}_k, t_k) - 2^{C}H_2(\mathcal{Y}_{k-1}, t_{k-1}) \right. \\ \left. + {}^{C}H_2(\mathcal{Y}_{k-2}, t_{k-2}) \right] \Delta \\ \mathcal{Y}(t_1) + \begin{cases} \frac{1-\varpi}{ABC(\varpi)} {}^{ABC}H_2(\mathcal{Y}_n, t_n) + \frac{\varpi}{ABC(\varpi)} \frac{(\delta t)^{\varpi-1}}{\Gamma(\varpi+1)} \sum\limits_{k=i+3}^{n} \left[{}^{ABC}H_2(\mathcal{Y}_{k-2}, t_{k-2}) \right] \Pi \\ + \frac{\varpi}{ABC(\varpi)} \frac{(\delta t)^{\varpi-1}}{\Gamma(\varpi+2)} \sum\limits_{k=i+3}^{n} \left[{}^{ABC}H_2(\mathcal{Y}_{k-1}, t_{k-1}) + ABC H_2(\mathcal{Y}_{k-2}, t_{k-2}) \right] \Sigma \\ + \frac{\varpi}{ABC(\varpi)} \frac{\varpi(\delta t)^{\varpi-1}}{\Gamma(\varpi+3)} \sum\limits_{k=i+3}^{n} \left[{}^{ABC}H_2(\mathcal{Y}^k, t_k) - 2^{ABC}H_2(\mathcal{Y}_{k-1}, t_{k-1}) \right. \\ \left. + {}^{ABC}H_2(\mathcal{Y}_{k-2}, t_{k-2}) \right] \Delta. \end{cases} \end{cases} \tag{16}$$

$$\mathcal{Z}(t_{n+1})) = \begin{cases} \mathcal{Z}_0 + \begin{cases} \frac{(\Delta t)^{\varpi-1}}{\Gamma(\varpi+1)} \sum\limits_{k=2}^{i} \left[{}^{C}H_3(\mathcal{Z}_{k-2}, t_{k-2}) \right] \Pi + \frac{(\Delta t)^{\varpi-1}}{\Gamma(\varpi+2)} \sum\limits_{k=2}^{i} \left[{}^{C}H_3(\mathcal{Z}_{k-1}, t_{k-1}) \right. \\ \left. - {}^{C}H_3(\mathcal{Z}_{k-2}, t_{k-2}) \right] \Sigma + \frac{\varpi(\Delta t)^{\varpi-1}}{2\Gamma(\varpi+3)} \sum\limits_{k=2}^{i} \left[{}^{C}H_3(\mathcal{Z}_k, t_k) - 2^{C}H_3(\mathcal{Z}_{k-1}, t_{k-1}) \right. \\ \left. + {}^{C}H_3(\mathcal{Z}_{k-2}, t_{k-2}) \right] \Delta \\ \mathcal{Z}(t_1) + \begin{cases} \frac{1-\varpi}{ABC(\varpi)} {}^{ABC}H_3(\mathcal{Z}_n, t_n) + \frac{\varpi}{ABC(\varpi)} \frac{(\delta t)^{\varpi-1}}{\Gamma(\varpi+1)} \sum\limits_{k=i+3}^{n} \left[{}^{ABC}H_3(\mathcal{Z}_{k-2}, t_{k-2}) \right] \Pi \\ + \frac{\varpi}{ABC(\varpi)} \frac{(\delta t)^{\varpi-1}}{\Gamma(\varpi+2)} \sum\limits_{k=i+3}^{n} \left[{}^{ABC}H_3(\mathcal{Z}_{k-1}, t_{k-1}) + ABC H_3(\mathcal{Z}_{k-2}, t_{k-2}) \right] \Sigma \\ + \frac{\varpi}{ABC(\varpi)} \frac{\varpi(\delta t)^{\varpi-1}}{\Gamma(\varpi+3)} \sum\limits_{k=i+3}^{n} \left[{}^{ABC}H_3(\mathcal{Z}^k, t_k) - 2^{ABC}H_3(\mathcal{Z}_{k-1}, t_{k-1}) \right. \\ \left. + {}^{ABC}H_3(\mathcal{Z}_{k-2}, t_{k-2}) \right] \Delta. \end{cases} \end{cases} \tag{17}$$

$$\mathcal{U}(t_{n+1})) = \begin{cases} \mathcal{U}_0 + \begin{cases} \frac{(\Delta t)^{\varpi-1}}{\Gamma(\varpi+1)} \sum\limits_{k=2}^{i} \Big[{}^{C}H_4(\mathcal{U}_{k-2}, t_{k-2})\Big]\Pi + \frac{(\Delta t)^{\varpi-1}}{\Gamma(\varpi+2)} \sum\limits_{k=2}^{i} \Big[{}^{C}H_4(\mathcal{U}_{k-1}, t_{k-1}) \\ -{}^{C}H_4(\mathcal{U}_{k-2}, t_{k-2})\Big]\sum + \frac{\varpi(\Delta t)^{\varpi-1}}{2\Gamma(\varpi+3)} \sum\limits_{k=2}^{i} \Big[{}^{C}H_4(\mathcal{U}_k, t_k) - 2{}^{C}H_4(\mathcal{U}_{k-1}, t_{k-1}) \\ +{}^{C}H_4(\mathcal{U}_{k-2}, t_{k-2})\Big]\Delta \end{cases} \\ \mathcal{U}(t_1) + \begin{cases} \frac{1-\varpi}{ABC(\varpi)}{}^{ABC}H_4(\mathcal{U}_n, t_n) + \frac{\varpi}{ABC(\varpi)} \frac{(\delta t)^{\varpi-1}}{\Gamma(\varpi+1)} \sum\limits_{k=i+3}^{n} \Big[{}^{ABC}H_4(\mathcal{U}_{k-2}, t_{k-2})\Big]\Pi \\ + \frac{\varpi}{ABC(\varpi)} \frac{(\delta t)^{\varpi-1}}{\Gamma(\varpi+2)} \sum\limits_{k=i+3}^{n} \Big[{}^{ABC}H_4(\mathcal{U}_{k-1}, t_{k-1}) + {}^{ABC}H_4(\mathcal{U}_{k-2}, t_{k-2})\Big]\sum \\ + \frac{\varpi}{ABC(\varpi)} \frac{\varpi(\delta t)^{\varpi-1}}{\Gamma(\varpi+3)} \sum\limits_{k=i+3}^{n} \Big[{}^{ABC}H_4(\mathcal{U}^k, t_k) - 2{}^{ABC}H_4(\mathcal{U}_{k-1}, t_{k-1}) \\ +{}^{ABC}H_4(\mathcal{U}_{k-2}, t_{k-2})\Big]\Delta. \end{cases} \end{cases} \tag{18}$$

Here

$$\Delta = \begin{bmatrix} (1+n-k)^{\varpi}\Big(2(n-k)^2 + (3\varpi+10)(n-k) + 2\varpi^2 + 9\varpi + 12\Big) \\ -(n-k)\Big(2(n-k)^2 + (5\varpi+10)(-k+n) + 6\varpi^2 + 18\varpi + 12\Big) \end{bmatrix},$$

$$\sum = \begin{bmatrix} (1+n-k)^{\varpi}\Big(3 + 2\varpi - k + n\Big) \\ -(n-k)\Big(n-k+3\varpi+3\Big) \end{bmatrix},$$

$$\Delta = \begin{bmatrix} (1+n-k)^{\varpi} - (n-k)^{\varpi} \end{bmatrix}.$$

and

$$\begin{aligned} {}^{C}H_1(\mathcal{X},\mathcal{Y},\mathcal{Z},\mathcal{U},t) &= {}^{ABC}H_1(\mathcal{X},\mathcal{Y},\mathcal{Z},\mathcal{U},t) = \lambda_h - \alpha_1\beta_1\mathcal{X}\mathcal{U} - \delta_1\mathcal{X}, \\ {}^{C}H_2(\mathcal{X},\mathcal{Y},\mathcal{Z},\mathcal{U},t) &= {}^{ABC}H_2(\mathcal{X},\mathcal{Y},\mathcal{Z},\mathcal{U},t) = \alpha_1\beta_1\mathcal{X}\mathcal{U} - \delta_1\mathcal{Y}, \\ {}^{C}H_3(\mathcal{X},\mathcal{Y},\mathcal{Z},\mathcal{U},t) &= {}^{ABC}H_3(\mathcal{X},\mathcal{Y},\mathcal{Z},\mathcal{U},t) = \lambda_m - \alpha_2\beta_2\mathcal{Y}\mathcal{Z} - \delta_2\mathcal{Z}, \\ {}^{C}H_4(\mathcal{X},\mathcal{Y},\mathcal{Z},\mathcal{U},t) &= {}^{ABC}H_4(\mathcal{X},\mathcal{Y},\mathcal{Z},\mathcal{U},t) = \alpha_2\beta_2\mathcal{Y}\mathcal{Z} - \delta_2\mathcal{U}. \end{aligned}$$

5 Experimental Results and Discussion: Numerical Performances of the Piecewise Global Fractional Derivatives for Zika Virus Infection

This section is concerned with the numerical scheme proposed by this study for simulating the considered model from which the simulation will be carried out over the time interval $[0, T]$, as shall be split into two sub-intervals: $[0, t_1)$ and $(t_1, T]$. To demonstrate the effectiveness of the numerical scheme of the study,

Table 1. Different numerical values for the considered model (1) with Data-I [22].

Symbol	value	Symbol	value	Symbol	value
$\mathcal{X}_0$	100	λ_h	1.2	α_2	0.005
$\mathcal{Y}_0$	60	λ_m	0.3	β_2	0.0003
$\mathcal{Z}_0$	40	α_1	0.0004	δ_1	0.004
$\mathcal{U}_0$	20	β_1	0.02	δ_2	0.0014

Table 2. Initial and parameters numerical values for ZV disease model (1) Data-II [18].

Symbol	value	Symbol	value	Symbol	value
$\mathcal{X}_0$	400	λ_h	1.2	α_2	0.005
$\mathcal{Y}_0$	100	λ_m	0.3	β_2	0.0003
$\mathcal{Z}_0$	600	α_1	0.0004	δ_1	0.004
$\mathcal{U}_0$	140	β_1	0.02	δ_2	0.0014

two different datasets have been used: the first data set is taken from [22], and the second one is from [18]. The data for both datasets are shown in Tables 1 and 2, respectively.

Numerical simulations are at stake for Data-I at various fractional orders, which are presented in Figs. 1a through 1d. In order to simulate the system of equations, we have utilized the idea of piecewise fractional derivatives, which are defined over the interval $[0, T]$. The graphical presentations are arranged and designed in the Matlab through which all the analysis and applications are conducted [23].

Caputo derivatives have specifically been utilized for the simulations on $[0, t_1]$, while we have employed ABC derivative representations have been employed for the simulations over $[t_1, T]$, where $t_1 = 25$ and $T = 50$. The simulations presented are based on different fractional orders. As can be seen from the results, the healthy population increases due to the high recruitment rate, while the infected human population decreases as healthy individuals enter the population. The same trend is observed for healthy and infected mosquitoes at various fractional orders, indicating that the disease is under control.

The graphical representation of the piecewise derivative for the two sub-intervals, utilizing two distinct concepts of fractional derivatives provides certain findings, and this representation exhibits a bending or cut, illustrated by the arrow, which can aid in understanding the crossover behavior phenomenon. Such a behavior is frequently witnessed when an infection undergoes sudden decay or growth, beyond the explanatory capacity of deterministic methods.

Simulations using Data-II have also been carried out, as presented in Figs. 2a to 2d. We have employed the notion of piecewise fractional derivative on the interval $[0, T]$, where Caputo derivative simulations were performed on $[0, t_1]$,

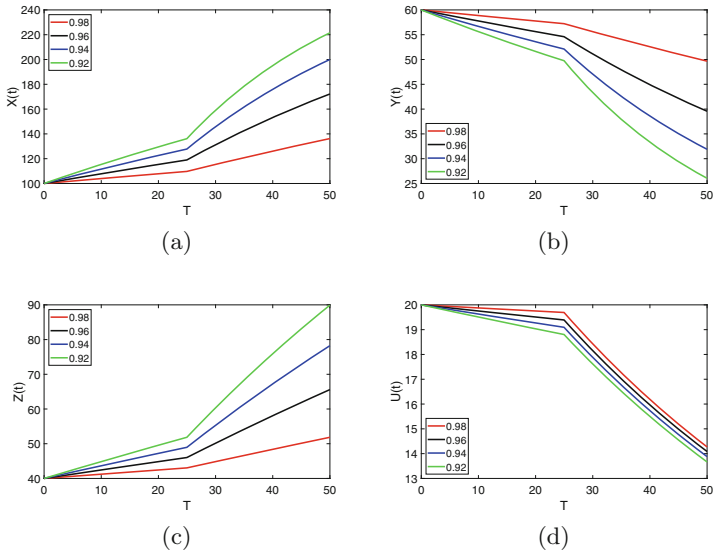


Fig. 1. Dynamics of $\mathcal{X}, \mathcal{Y}, \mathcal{Z}, \mathcal{U}$ classes at various fractional order ϖ for the set of Data-I on sub interval $[0, t_1]$ and $[t_1, T]$ of $[0, T]$, where $t_1 = 25$, $T = 50$.

and ABC derivative representations were illustrated over $[t_1, T]$. Two scenarios, namely $t_1 = 25$ and $T = 50$, and $t_1 = 60$ and $T = 120$ have been taken into consideration in this study. In these simulations, we observe that the healthy population initially declines but eventually stabilizes. In contrast, the infectious human population initially grows but eventually stabilizes. To clarify, it has been found that the identical behavior is exhibited by both healthy and infected mosquitoes, across various fractional orders, which suggests that the infection is not initially under control, but can potentially be managed through appropriate and effective treatment and care strategies and interventions.

As with the previous simulations, we have examined the piecewise derivative graphical representation for the two sub-intervals using two different concepts of fractional orders. As demonstrated by the arrow, the graphical representation displays bends or cuts in the middle of the curves, and consequently, these features aid in elucidating the crossover behavior observed in the simulations.

6 Conclusion and Future Directions

Formulating fractional order compartment models through the consideration of differential equations based on the underlying stochastic processes can point towards a systematic approach to ensure predictive accuracy allowing that the model remains plausible at all times. Such a scheme is capable of providing a convenient interpretation and feasible design with regard to all the parameters and partitions of the model. Towards these multi-stage processes, this study

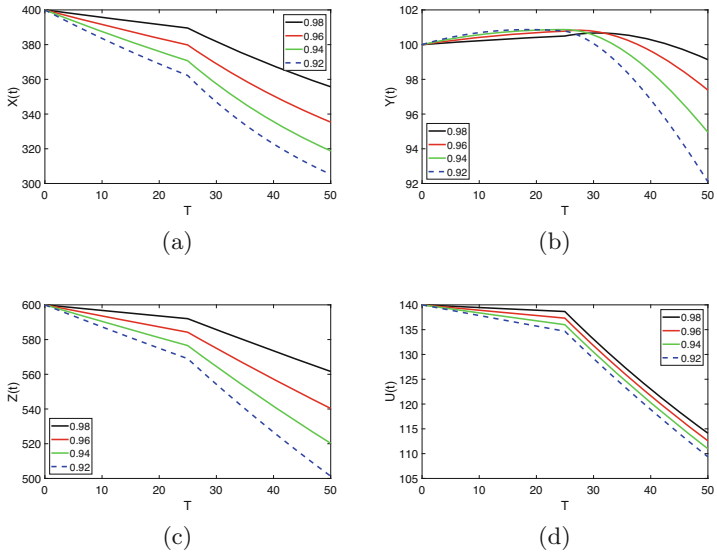


Fig. 2. Dynamics of $\mathcal{X}, \mathcal{Y}, \mathcal{Z}, \mathcal{U}$ classes at various fractional order ϖ for the set of Data-II on sub interval $[0, t_1]$ and $[t_1, T]$ of $[0, T]$.

aims to introduce new concepts of fractional calculus that manifest crossover effects in dynamical models. To this end, piecewise global fractional derivatives in sense of Caputo and Atangana-Baleanu-Caputo (ABC) have been utilized, and they are applied to formulate the Zika Virus (ZV) disease model. In order to have a predictive analysis of the behavior of the model, the strain is divided into two subintervals and the piecewise behavior is investigated. Thereafter, the fixed point theory of Schauder and Banach is employed for proving the existence and uniqueness of at least one solution in both senses for the considered problem. With respect to the numerical simulations based on the data, Newton interpolation formula has been modified and extended for the considered nonlinear system in the study where graphical presentations and illustrative examples are based on the data for various multi-compartments of the systems with respect to the applicable real-world data for different fractional orders. The obtained results verify that increasing the fractional order results in a greater crossover effect, which is clearly observable, and reducing the fractional order reduces the abrupt changes. This effect cannot be demonstrated using ordinary fractional order or stochastic differential equations. Based on the impact of fractional order reducing the abrupt changes, the results obtained from the study demonstrate and also validate that increasing the fractional order yields a greater crossover effect, as evident from the observed data, which is critical for the effective management and control of abrupt changes like infectious diseases, viruses, among many more unexpected dynamic and nonlinear phenomena in chaotic, uncertain and transient circumstances. Taken together, as future directions, the established analysis can be extended to more complex dynamical problems of fractional order

involving piecewise differential equations. The developed models with the proposed scheme can be used for other illnesses and diseases as well as pertinent data for the estimation, prediction, management as well as control purposes in the ever-evolving global landscape.

References

1. Zika virus, World Health Organization (2015). http://www.who.int/mediacentre/factsheets/zika/en/
2. Calvet, G., Aguiar, R.S., Melo, A.S.O., et al.: Detection and sequencing of Zika virus from amniotic fluid of fetuses with microcephaly in Brazil: a case study. Lancet Infect. Dis. **16**, 653–660 (2016)
3. Perkins, T.A., Siraj, A.S., Ruktanonchai, C.W., et al.: Model-based projections of Zika virus infections in childbearing women in the Americas. Nat. Microbiol. **1**, 16126 (2016)
4. Kucharski, A.J., Funk, S., Eggo, R.M.M., et al.: Transmission dynamics of Zika virus in island populations: a modelling analysis of the 2013–14 French Polynesia outbreak. PLoS Neglect. Trop. D. **10**, 38588 (2016)
5. Bonyah, E., Okosun, K.O.: Mathematical modeling of Zika virus. Asian Pac. J. Trop. Dis. **6**, 637–679 (2016)
6. Bonyah, E., Khan, M.A., Okosun, K.O., et al.: A theoretical model for Zika virus transmission. PLoS ONE **12**, 1–26 (2017)
7. Machado, J.T., Kiryakova, V., Mainardi, F.: Recent history of fractional calculas. Commun. Nonl. Sci. Num. Simul. **16**(3), 1140–1153 (2011)
8. Hilfer, R.: Threefold Introduction to Fractional Derivatives, Anomalous Transport: Foundations and Applications. Germany (2008)
9. Agarwal, R.P., Lakshmikantham, V., Nieto, J.J.: On the concept of solution for fractional differential equations with uncertainty. Nonlinear Anal.: Theory Methods Appl. **72**(6), 2859–2862 (2010)
10. Grace, S., Agarwal, R., Wong, P., Zafer, A.: On the oscillation of fractional differential equations. Fractional Calculus Appl. Anal. **15**(2), 222–231 (2012)
11. Xu, C., Liao, M., Li, P., Yuan, S.: Impact of leakage delay on bifurcation in fractional-order complex-valued neural networks. Chaos Solitons Fractals **142**, 110535 (2021)
12. Liu, X., Rahmamn, M.U., Ahmad, S., Baleanu, D., Anjam, Y.N.: A new fractional infectious disease model under the non-singular Mittag-Leffler derivative. Waves Random Complex Media 1–27 (2022)
13. Riaz, M.B., Awrejcewicz, J., Rehman, A.U.: Functional effects of permeability on Oldroyd-B fluid under magnetization: a comparison of slipping and non-slipping solutions. Appl. Sci. **11**(23), 11477 (2021)
14. Riaz, M.B., Saeed, S.T.: Comprehensive analysis of integer-order, Caputo-Fabrizio (CF) and Atangana-Baleanu (ABC) fractional time derivative for MHD Oldroyd-B fluid with slip effect and time dependent boundary condition. Discret. Continuous Dyn. Syst.-S **14**(10), 3719 (2021)
15. Rahman, M.U., Arfan, M., Shah, Z., Kumam, P., Shutaywi, M.: Nonlinear fractional mathematical model of tuberculosis (TB) disease with incomplete treatment under Atangana-Baleanu derivative. Alex. Eng. J. **60**(3), 2845–2856 (2021)
16. Rahman, M.U., Alhawael, G., Karaca, Y.: Compartmental analysis of middle eastern respiratory syndrome coronavirus model under fractional operator with next-generation matrix methods. Fractals (2023)

17. Baleanu, D., Ghassabzade, F.A., Nieto, J.J., Jajarmi, A.: On a new and generalized fractional model for a real cholera outbreak. Alex. Eng. J. **61**(11), 9175–9186 (2022)
18. Khan, M.A., Ullah, S., Farhan, M.: The dynamics of Zika virus with Caputo fractional derivative. AIMS Math. **4**(1), 134–146 (2019)
19. Atangana, A., Baleanu, D.: New fractional derivatives with non-local and non-singular kernel. Therm. Sci. **20**(2), 763–769 (2016)
20. Karaca, Y.: Computational complexity-based fractional-order neural network models for the diagnostic treatments and predictive transdifferentiability of heterogeneous cancer cell propensity. Chaos Theory Appl. **5**(1), 34–51 (2023)
21. Atangana, A.: Extension of rate of change concept: from local to nonlocal operators with applications. Results Phys. **19**, 103515 (2020)
22. Atangana, A., Araz, S.I.: New concept in calculus: piecewise differential and integral operators. Chaos Solitons Fractals **145**, 110638 (2021)
23. MATLAB, 2022 version 9.12.0 (R2022a). The Math-Works Inc., Natick, Massachusetts